



Aalborg Universitet

AALBORG UNIVERSITY
DENMARK

Hybrid islanding detection method by using grid impedance estimation in parallel-inverters-based microgrid

Ghzaiel, Walid ; Jebali-Ben Ghorbal, Manel ; Slama-Belkhodja, Ilhem ; Guerrero, Josep M.

Published in:
Proceedings of ELECTRIMACS 2014

Publication date:
2014

Document Version
Early version, also known as pre-print

[Link to publication from Aalborg University](#)

Citation for published version (APA):
Ghzaiel, W., Jebali-Ben Ghorbal, M., Slama-Belkhodja, I., & Guerrero, J. M. (2014). Hybrid islanding detection method by using grid impedance estimation in parallel-inverters-based microgrid. In *Proceedings of ELECTRIMACS 2014* (pp. 433-438). IMACS.

General rights

Copyright and moral rights for the publications made accessible in the public portal are retained by the authors and/or other copyright owners and it is a condition of accessing publications that users recognise and abide by the legal requirements associated with these rights.

- Users may download and print one copy of any publication from the public portal for the purpose of private study or research.
- You may not further distribute the material or use it for any profit-making activity or commercial gain
- You may freely distribute the URL identifying the publication in the public portal -

Take down policy

If you believe that this document breaches copyright please contact us at vbn@aub.aau.dk providing details, and we will remove access to the work immediately and investigate your claim.

HYBRID ISLANDING DETECTION METHOD BY USING GRID IMPEDANCE ESTIMATION IN PARALLEL-INVERTERS-BASED MICROGRID

Walid Ghzaïel¹, Manel Jebali-Ben Ghorbal², Ilhem Slama-Belkhodja³ and Josep M. Guerrero⁴

123 Université de Tunis El Manar, ENIT-L.S.E, BP 37-1002, Tunis le Belvédère, Tunis, Tunisie.

4 Aalborg University, Dept. Energy Technology, 9220 Aalborg, Denmark

E-mail: ghzaïel.walid@gmail.com, maneljebali2001@yahoo.fr, ilhem.slama@enit.rnu.tn, joz@et.aau.dk

Abstract –This paper presents a hybrid islanding detection algorithm integrated on the distributed generation unit more close to the point of common coupling of a Microgrid based on parallel inverters where one of them is responsible to control the system. The method is based on resonance excitation under grid impedance variation. Firstly, grid impedance variation will be detected easily and rapidly by sensing any abrupt grid current variation. Then, the closest inverter to the grid will excite the resonance to detect the grid fault by using virtual resistance, in order to extract the grid impedance parameters, both resistive and inductive parts, from the injected resonance frequency determination. Finally, the inverter will disconnect the microgrid from the faulty grid and reconnect the parallel inverter system to the controllable distributed system in order to ensure high power quality. This paper shows that grid impedance variation detection-estimation can be an efficient method for islanding detection in microgrid systems. Theoretical analysis and simulation results are presented to validate the proposed method.

Keywords –Microgrid, islanding, Grid impedance variation, resonance excitation, droop control method, virtual resistance.

1. INTRODUCTION

In the last decade, the electric power production is based on the oil and fossil fuels around the world. Recently, the increase of energy demand is boosting the attention towards the power generation systems based on renewable sources (sun and wind) named Distributed generation System (DGS), often localised near the loads. These systems reduce the losses of long-distance transmission cables and environmental pollution. The need of integrating different types of DG, such as diesel engines, micro-turbines, fuel cells, wind turbines and photovoltaic source, into the electrical infrastructure to make it efficient, reliable and intelligent is given the idea of a Microgrid (MG) concept in order to coordinate between the different types of DGSs. MG is defined as low voltage intelligent distribution networks consisting of various distributed generators, storage devices, local loads and parallel inverters. It can operate autonomously or in interaction with the utility grid [1]. The connection and disconnection of MG depends on the electrical power quality exchanged with the grid at the point of common coupling PCC (Pre-planned islanded) and the existing of blackout (Non-planned islanded) [2].

Hence, a reliable islanding detection method should be set in order to detect islanding conditions as fast as possible under all grid conditions (stiff or weak). Thus, several methods have been proposed to estimate the grid impedance, according to the European ENS standard an increase of 0.5Ω should lead to grid disconnection within 5s [3], in the

literature in order to detect the islanding condition [3]-[4]-[5]. These methods can mainly classify into passive and active method.

However, in [5], passive methods cannot operate in Non-Detection Zone (NDZ). Besides, the voltage at PCC depends not only on the grid impedance variation but also on the load impedance variation or load harmonic injection.

Unlike, the injection of predefined harmonic in case of active methods is more efficient. But, this step should be precedent by the grid impedance variation detection step to avoid the periodic perturbation injection. In this sense, a novel hybrid islanding detection method based on grid current measurements and a resonance excitation is proposed in this paper. This method is able to detect islanding conditions under any worst condition and even in NDZ, where other methods failed [6]. This method is easy to apply in only DGS establish. But, in MG that comprises parallel inverters connected to the grid, the method application is more difficult because of the proper resonance frequency of each DG+grid impedance system. The proposed solution used in this paper to avoid this situation and to improve the power quality is extracted from the structure of parallel inverters connected to double grid. This algorithm avoids reducing the MG power quality during the resonance excitation.

This paper is organized as follows. The double grid-connected MG structure and the proposed MG control structure are being described in section 2. The proposed improved grid impedance estimation is presented and discussed in section 3 with the different algorithm steps. Finally, in section 4 simulation results are given.

2. MICROGRID

As aforementioned in section 1, MG is formed by different DGSs types connected in parallel to the main grid modelled by resistive inductive branch in series with an ideal voltage source. In this paper, the parallel DGSs is modelled by a three-phase inverters connected to the common AC bus through an LCL-filter to better reducing the switching harmonics in order to respect the norm (THD<5%).

2.1. MICROGRID CONNECTED TO DOUBLE GRID

The penetration of the DGSs is boosting the appearance of many DGSs grid-connection structure to ensure the continuity of power exchange between MG based on parallel DGSs and utility grid. One of the connection structures is the existence of double grid connected through an intelligent bypass switch (IBS) to the common AC bus. Fig. 1 presents a double grid-connected MG structure.

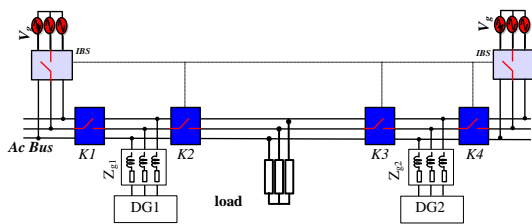


Fig. 1. Microgrid connected to double grid

Indeed, the parallel inverters are usually connected only to one grid. In case of fault appearance in one of the grids, the switches $K_{i=1,6}$ close and open according to the grid fault in manner to make the loads and DGSs connected to healthy grid. The proposed hybrid islanding detection method is based on resonance excitation. However, resonance of parallel inverters with different line impedance decreases the MG power quality and can damage certain critical loads. As solution, an inverter with loads can still connected to the healthy grid where the other DGS excites the resonance to determine the grid impedance of the faulty grid. Hence, the estimated impedance values helps keeping the grid connected or disconnect it from the utility faulty grid.

2.2. PROPOSED MICROGRID STRUCTURE

Instead of double grid-connected, the proposed MG control structure is based on just only grid as usually worked on. Controllable DGS, such as gas engine, diesel generator and distributed storage system, acts as a second grid source connected to parallel inverters in order to support the voltage and frequency in islanded mode [7]. The parallel inverters act as current sources. The system composed on controllable DGS, parallel inverters

and loads is connected to the grid closest DGS through a switch K1 and all the system is connected to the grid through IBS as depicted in Fig.2. In fact, grid impedance variation challenges the AC bus interfacing inverter control which leads to poor power quality. In this way, the switch K1 should be opened immediately under grid impedance variation detection to avoid resonance problems in MG caused by the interaction between system and grid. Hence, controllable DG will supply together with parallel inverters the loads. The closest DG will execute the algorithm of grid impedance parameters determination. Different possible scenarios are presented in Table I.

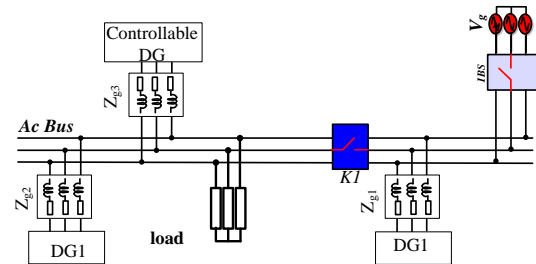


Fig.2 Proposed Structure

I. Proposed MG scenarii

IBS	K1	Scenario
Closed	Closed	Connected MG
Closed	Opened	Connected DG
Opened	Closed	Islanded MG

3. PROPOSED MICROGRID CONTROL STRATEGY

In grid-connected mode, parallel DGSs behave like a current source with current source inverters (CSI) used for PV and WT that require (MPPT) algorithm in order to inject the maximum power to the grid and both frequency and voltage are supported by the grid. Only the controllable DGS acts as a voltage source, using voltage source inverter (VSI), where its reference is the grid voltage and frequency [7]. In islanded mode and during the hybrid islanding detection algorithm application explained next, the controllable DGS will change its references while the parallel DGSs still working as current sources.

3.1. HYBRID ISLANDING METHOD

The islanding detection method used in this paper, implemented in the closest grid-connected DGS, is composed on:

Passive part: based on temporal redundancies of grid current measurements. This method is widely

used and its efficiency in fault detection and isolation of faulty sensor in electrical drives (FDI) was proven [8]. Its principle consists on the detection of any abrupt variation between two consecutive grid current measurements. This variation will be depicted as a residual with different amplitude level. Indeed, in healthy conditions, with no grid impedance variation, the residual noted Res_{igk} is lower than a predefined threshold. As the grid impedance varies, this residual increases significantly. Hence, a spike will be presented at the instant of the grid fault (grid impedance variation). The residual expressions are given by (1) and (2).

$$Re s_{igk} = r_k + r_{k-1} + r_{k-2} \quad (1)$$

$$r_k = |i_{gk} - 2i_{gk-1} + i_{gk-2}| \quad (2)$$

Where i_{gk} , i_{gk-1} and i_{gk-2} are the consecutive measured current at kTa , $(k-1)Ta$ and $(k-2)Ta$ respectively. The threshold responsible on taken the decision of grid fault existence is expressed as

$$\varepsilon = 3\omega^2 Ta^2 I_m \quad (3)$$

$$I_m = \frac{V_{PCCm} - V_{gm}}{|Z_g|} \quad (4)$$

Where V_{PCCm} is the maximum voltage at PCC, V_{gm} is the maximum grid voltage and τ_s ($\omega = 2\pi / \tau_s$) is the system time constant.

Active part: needed to estimate the grid impedance parameters value under grid fault. The adopted method is based on resonance excitation. As proven in [6], the system resonance frequency depends on the grid impedance, especially on the inductive part of the grid impedance. The resonance frequency of closest DGS presented in Fig. 3(I) is expressed as follows:

$$f_{res} = \frac{1}{2\pi} \sqrt{\frac{L_1 + L_2 + L_{line1} + L_g}{L_1(L_2 + L_{line1} + L_g)C_f}} \quad (5)$$

The inductive part of the grid impedance can be deduced from the resonance frequency by applying the Fast Fourier transformation (FFT). Consequently, the grid inductance can be deduced as follows:

$$L_g = \frac{(L_1 + L_2 + L_{line1}) - (4\pi^2 L_1(L_2 + L_{line1})C_f f_{res}^2)}{(4\pi^2 L_1 C_f f_{res}^2 - 1)} \quad (6)$$

The excitation is based on virtual damping resistance noted R_v that used for both drive the system to the resonance then extract the resonance frequency and improve the power quality by damping the resonance effect produced by non-

linear load. The principle of the method consists on taking a high proportional gain at the beginning, and then reducing the virtual resistance gradually until reaching the resonance. Theoretical analysis is well explained in [6]. The resistive value, R_g , can be deduced from the residual and L_g as follows:

$$R_g = \sqrt{\frac{9\omega^4 Ta^4}{\varepsilon^2} (V_{PCCm} - V_{gm})^2 - (\omega L_g)^2} \quad (7)$$

The proportional resonant (**P+R**) controller is adopted to control the **DGS** output current due to its high regulation capability and its harmonics suppression effect [9]. The transfer functions of a non-ideal **P+R** controller used given by:

$$G_{i_{ex}}(s) = k_{pex} + \frac{k_{rex} s}{s^2 + 2\omega_c s + \omega^2} + \sum_{h=5,7,11} \frac{k_{rexh} s}{s^2 + 2\omega_c s + \omega_h^2} \quad (8)$$

k_{pex} is the proportional gain responsible on the system dynamic while k_{rex} is the resonant gain responsible on reducing the steady-state error. ω , ω_h and ω_c are respectively the fundamental frequency, the harmonic frequencies and the cut-off frequency used for frequency fluctuation reducing.

3.2. CONTROLLABLE DG CONTROL

Indeed, active and reactive powers noted (P and Q) flowing from the controllable DGS, here modelled by the VSI+LC part-filter, to the grid through an inductor can be expressed as following [10],[11]:

$$P = \left(\frac{EV}{Z} \cos \phi - \frac{V^2}{Z}\right) \cos \theta + \frac{EV}{Z} \sin \phi \cos \theta \quad (9)$$

$$Q = \left(\frac{EV}{Z} \cos \phi - \frac{V^2}{Z}\right) \sin \theta - \frac{EV}{Z} \sin \phi \cos \theta \quad (10)$$

ϕ is the phase angle between the inverter output and the MG voltage (V_{PCC}), Z is the inductor impedance, E is the DGS capacitor voltage amplitude, V is the grid voltage amplitude and θ is the impedance angle. The droop method used to control the controllable DGS is based on two assumption, the first one is that the output impedance is purely inductive ($Z=X$, $\theta=90^\circ$), this assumption is carried out by grid-side inductance, where the second one is that the angle between the inverter output and the voltage is too small ($\phi=0$, $\cos \phi=1$). Based on these two assumptions, the equations (9) and (10) can be expressed as follows where integrator terms are added to improve the transient response of the system:

$$\phi = \phi^* - G_p(s)(P - P^*) \quad (11)$$

$$E = E^* - G_q(s)(Q - Q^*) \quad (12)$$

ϕ is the phase of the V_c^* , $\phi^* = \omega^* \int dt = \omega^* t$

Being

$$G_p(s) = \frac{m_I s + m}{s} \quad (13)$$

$$Gq(s) = \frac{n_I s + n}{s} \quad (14)$$

The active and reactive powers are calculated using the two next equations where low pass filter is used to attenuate the ripples:

$$P = \frac{\omega_f}{s + \omega_f} (Vc\alpha i\alpha + Vc\beta i\beta) \quad (15)$$

$$Q = \frac{\omega_f}{s + \omega_f} (Vc\beta i\alpha - Vc\alpha i\beta) \quad (16)$$

The three voltage reference is obtained from the output of the droop control stage as depicted in Fig.3 (II), where the voltage expression is given by:

$$Vc^* = E \sin(\omega t) \quad (17)$$

The voltage obtained at the droop control output and inverter current are both regulated by non-ideal P+R controller where its transfer function is presented by:

$$G_v(s) = k_{pv} + \frac{k_{rv} s}{s^2 + 2\omega_c s + \omega^2} + \sum_{h=5,7,11} \frac{k_{rvh} s}{s^2 + 2\omega_c s + \omega_h^2} \quad (18)$$

$$G_i(s) = k_{pi} + \frac{k_{ri} s}{s^2 + 2\omega_c s + \omega^2} + \sum_{h=5,7,11} \frac{k_{rih} s}{s^2 + 2\omega_c s + \omega_h^2} \quad (19)$$

It is worth to say that the voltage amplitude and the frequency are the grid voltage amplitude and frequency in scenario 1. The grid frequency is determined by SOGI-FLL characterized by its high efficiency under unbalance or perturbation as proven in literature [12].

4. SIMULATION

Simulations were carried out by using PSIM software. The proposed islanding detection method was described for detection and estimation of grid impedance variation is tested on a three phase controllable DGS inverter, three phase inverter DG2 and three phase inverter for the closest DG1 as described in Fig. 3. The system parameters used in simulations are shown in Table II, III and IV. In the second and third scenario, the voltage and frequency references are proposed by the system itself with $E=325V$ and $\omega=314.159$ rad/s.

Fig. 4 shows the resonance excitation after the appearance of residual peak due to grid impedance variation (from Z_g to Z_g+Z_d) at $t=1.24s$. It depicts also the inverse of the switch K1 pulse that is ON during resonance state in order to open the switch. Note that this pulse is related to gate non for software reasons.

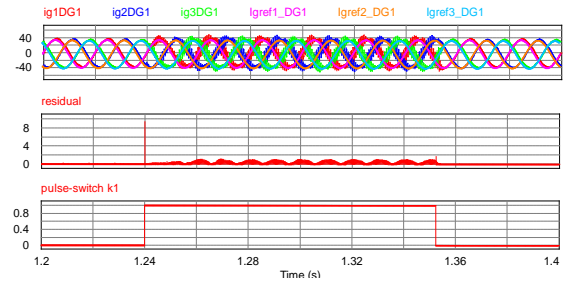


Fig. 4. Z_g variation detection & resonance excitation

Fig. 5 presents the DG1 output current and the grid current over and under resonance excitation. Under resonance excitation, the grid current is reduced due to the disconnection of the controllable DGS and DG2 that still acting as a sub-islanded MG. The LCL-filter capacitor voltage of the controllable DGS is depicted at down, where the resonance effect does not appear. Its amplitude follows the voltage amplitude obtained at the output of the droop control algorithm noted by E-reference.

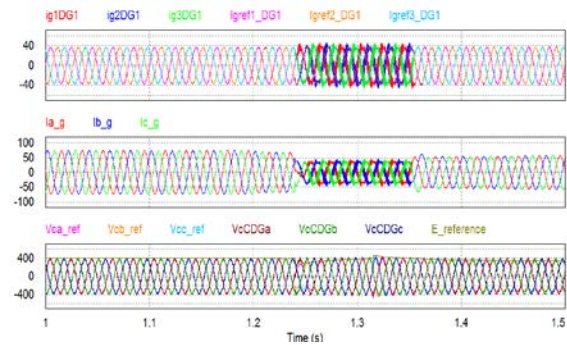


Fig. 5 resonance effect on grid & DGSs

In grid-connected controllable DGS, i.e no-grid impedance variation and K1 is closed, the system proposes its power reference, while in scenario 2 under resonance excitation, the loads will demand the needed power. Hence the active and reactive power references should be set to be null. This phenomenon is showed in Fig. 6.

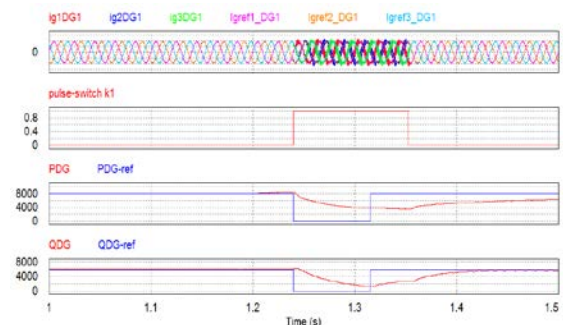


Fig. 6. Power control under/over resonance

As presented in the large Fig. 3, linear resistive, linear inductive and non-linear loads are connected to the AC bus at different times to show the effect of abrupt load variation and the polluted load on the

islanding detection method. Fig. 7 depicts that the proposed islanding detection method doesn't have any negative effect on the load current.

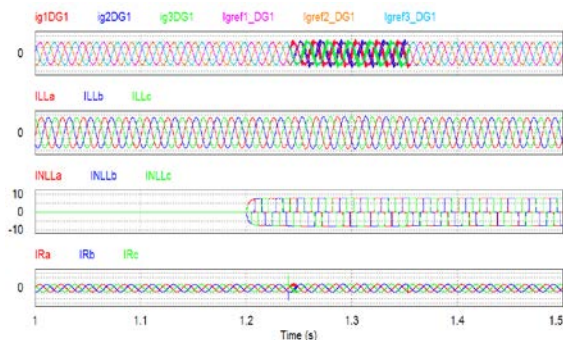


Fig. 7. Loads power under resonance excitation

CONCLUSION

Future intelligent grid aims to improve power quality and ensure the service continuity. In this sense, hybrid islanding detection method implemented in specific MG control strategy has been presented in this paper. The method is based on grid impedance estimation by LCL-filter resonance excitation using virtual resistance and was implemented on the closest DG control structure. During resonance excitation and in islanded mode, controllable DG was used to support the frequency and voltage of MG while the parallel inverters act as current sources. The proposed algorithm is a proper solution for both well islanding detection and maintaining the high MG power quality when a heavy grid fault occurs.

ACKNOWLEDGEMENTS

This work was supported by the Tunisian Ministry of High Education and Research under Grant LSE-ENIT-LR 11ES15.

REFERENCES

- [1] J. C. Vasquez, J. M. Guerrero, J. Miret, M. Castilla, and L. G. Vicuna "Hierarchical control of intelligent Microgrid" IEEE Industrial Electronics Magazine December 2010.
- [2] X. Wang, J. M. Guerrero and Zhe Chen "Control of Grid Interactive AC Microgrids" 2211 - 2216 Industrial Electronics (ISIE) 2010 IEEE
- [3] A.V. Timbus, P. Rodriguez, R. Teodorescu, M. Ciobotaru, "Line Impedance Estimation Using Active and Reactive Power Variations, " in *conf PESC.2007*, pp. 1273 -1279, 2007.
- [4] M. Ciobotaru, R. Teodorescu, and F. Blaabjerg, "On-line grid impedance estimation based on harmonic injection for grid-connected pv inverter," IEEE International Symposium on Industrial Electronics, pp. 2437 – 2442, IEEE-ISIE 2007.
- [5] A. Moallem, D. Yazdani, A. Bakhshai, P. Jain, "Frequency domain identification of the utility grid parameters for distributed power generation systems," *Twenty-Sixth Annual IEEE Applied Power Electronics Conference and Exposition (APEC)*, pp.965-969, Mar. 2011.
- [6] W. Ghzaïel, M. Jebali-Ben Ghorbal, I. Slama-Belkhdja and J. M. Guerrero "A Novel Grid Impedance Estimation Technique based on Adaptive Virtual Resistance Control Loop Applied to Distributed Generation Inverters". *Power Electronics and Applications (EPE), 2013 15th European Conference on*, pp. 1 – 10, 2013.
- [7] J. Rocabert, Gustavo M. S. Azevedo, A. Luna, J. M. Guerrero, J. I. Candela and P. Rodríguez "Intelligent Connection Agent for Three-Phase Grid-Connected Microgrids" *IEEE Transactions On Power Electronics*, Vol. 26, No. 10, pp. 2993 – 3005, OCTOBER 2011.
- [8] H. Berriri, M.W. Naouar, I. Slama-Belkhdj "Sensor Fault Tolerant Control For Wind Turbine Systems With Doubly Fed Induction Generator", *ELECTRIMACS 2011*, 6-8th June 2011, Cergy-Pontoise, France, 2011.
- [9] R. Teodorescu, F. Blaabjerg, M. Liserre, P.C. Loh "Proportional-resonant controllers and filters for grid-connected voltage-source converters" *IEEE Proc.-Electr. Power Appl.*, Vol. 153, No. 5, pp. 750 – 762 September 2006.
- [10] J. C. Vasquez J. M. Guerrero M. Savaghebi and R. Teodorescu: "Modeling, Analysis, and Design of Stationary Reference Frame Droop Controlled Parallel Three-Phase Voltage Source Inverters 8th International Conference on Power Electronics - ECCE Asia May 30-June 3
- [11] J.C. Vasquez, J.M. Guerrero, A. Luna, P. Rodriguez, R. Teodorescu : "Adaptive Droop Control Applied to Voltage-Source Inverters Operating in Grid-Connected and Islanded Modes, *IEEE Trans. on Industrial Electronics*, vol. 56, no. 10, pp. 4088 4096, Oct 2009.
- [12] P. Rodriguez, A. Luna, R. S. Munoz-Aguilar, I. Etxeberria-Otadui, R. Teodorescu and F. Blaabjerg "A Stationary Reference Frame Grid Synchronization System for Three-Phase Grid-Connected Power Converters under Adverse Grid Conditions" *IEEE Transactions On Power*

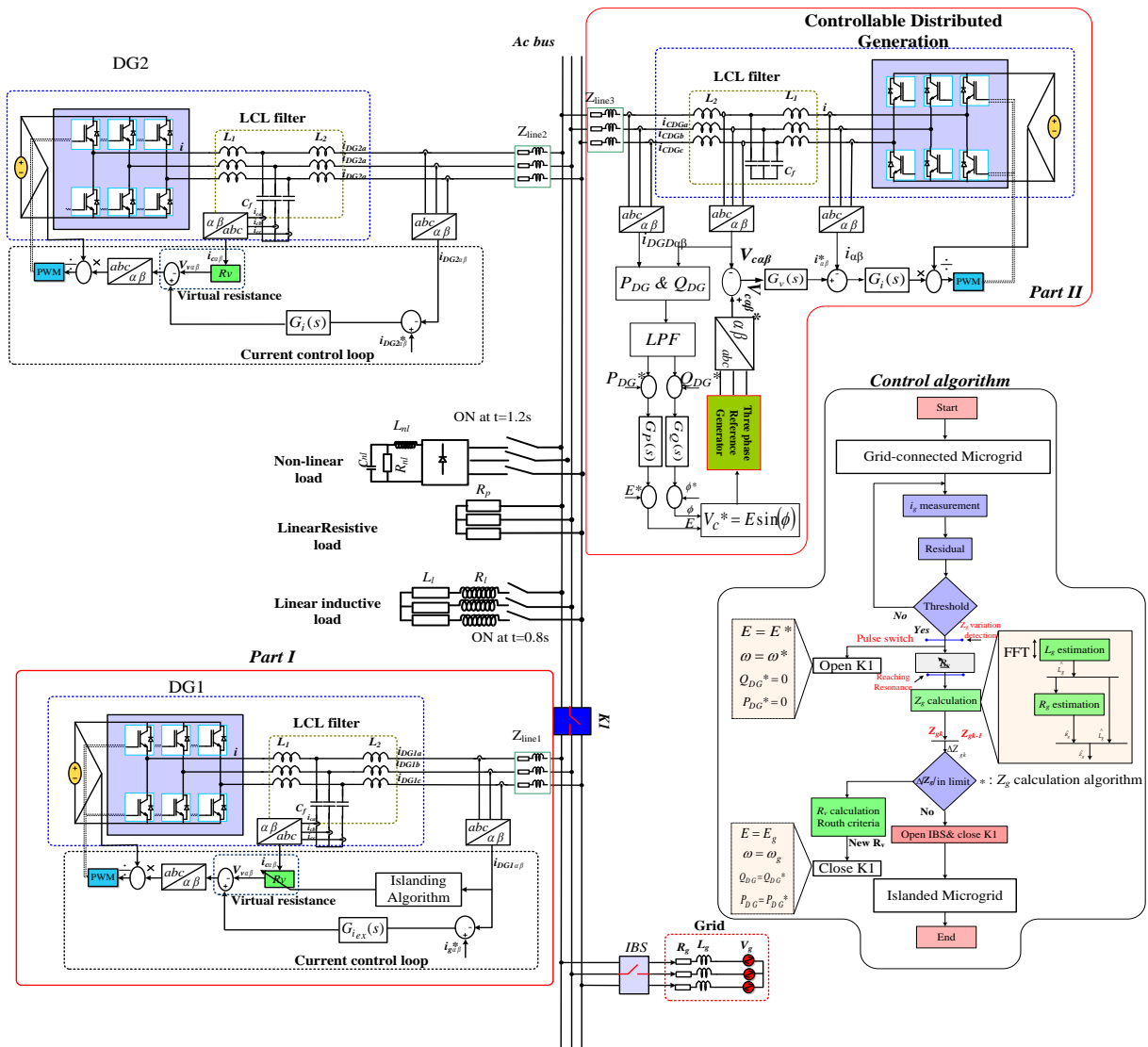


Fig. 3. Proposed Microgrid control structure

II. DGs parameters

P_{DG1}	P_{DG2}	P_{DG3}	$V_{DC}(V)$	f_{PWM}	L_1	L_2	C_f	Z_g	Z_d
10kW	8kW	8kW	650	10kHz	2mH	2mH	25 μ	0.4 Ω ,0.9mH	2mH

III Loads parameters

R_p	R_l	L_l	R_{nl}	L_{nl}	C_{nl}
55 Ω	128 Ω	0.204H	80 Ω	0.204H	2 μ F

IV. Control parameters

k_{pex}	k_{iex}	k_p	k_i	k_{pv}	k_{iv}	ω_c	ω_f	R_v	m	m_l	n	n_l	T_a
42	75000	2	180	0.9	50	4	8	35	0.00027	0.000028	0.02	0.12	5 μ